



Jensen, T. T., Hall, C., Potticary, J. L., Andrusenko, I., Gemmi, M., & Hall, S. R. (2019). An Experimental and Computational Study into the Crystallisation Propensity of 2nd Generation Sulflower. *Journal of the Chemical Society: Chemical Communications*, 55(97), 14586-14589 .  
<https://doi.org/10.1039/C9CC08346D>

Peer reviewed version

Link to published version (if available):  
[10.1039/C9CC08346D](https://doi.org/10.1039/C9CC08346D)

[Link to publication record in Explore Bristol Research](#)  
PDF-document

This is the author accepted manuscript (AAM). The final published version (version of record) is available online via Royal Society of Chemistry at <https://pubs.rsc.org/en/content/articlelanding/2019/cc/c9cc08346d#!divAbstract>. Please refer to any applicable terms of use of the publisher.

## University of Bristol - Explore Bristol Research

### General rights

This document is made available in accordance with publisher policies. Please cite only the published version using the reference above. Full terms of use are available:  
<http://www.bristol.ac.uk/red/research-policy/pure/user-guides/ebr-terms/>

# ChemComm

Chemical Communications

Accepted Manuscript

This article can be cited before page numbers have been issued, to do this please use: T. T. Jensen, C. Hall, J. Potticary, I. Andrusenko, M. Gemmi and S. Hall, *Chem. Commun.*, 2019, DOI: 10.1039/C9CC08346D.



This is an Accepted Manuscript, which has been through the Royal Society of Chemistry peer review process and has been accepted for publication.

Accepted Manuscripts are published online shortly after acceptance, before technical editing, formatting and proof reading. Using this free service, authors can make their results available to the community, in citable form, before we publish the edited article. We will replace this Accepted Manuscript with the edited and formatted Advance Article as soon as it is available.

You can find more information about Accepted Manuscripts in the [Information for Authors](#).

Please note that technical editing may introduce minor changes to the text and/or graphics, which may alter content. The journal's standard [Terms & Conditions](#) and the [Ethical guidelines](#) still apply. In no event shall the Royal Society of Chemistry be held responsible for any errors or omissions in this Accepted Manuscript or any consequences arising from the use of any information it contains.

## COMMUNICATION

## An Experimental and Computational Study into the Crystallisation Propensity of 2nd Generation Sulflower

Received 00th January 20xx,  
Accepted 00th January 20xxTorsten T Jensen<sup>a</sup>, Charlie L Hall<sup>a</sup>, Jason Potticary<sup>a</sup>, Iryna Andrusenko<sup>b</sup>, Mauro Gemmi<sup>b</sup>, Simon R Hall<sup>\*a</sup>

DOI: 10.1039/x0xx00000x

**The crystallisation propensity of the newly synthesised molecule persulfurated coronene has been investigated through a number of experimental methods. Electrostatic potential calculations and multi-molecular optimisations show that face-face interactions are far more favorable than edge-face interactions, severely restricting the ability of the molecule to crystallise.**

Amongst all known small organic molecules, rigid planar aromatics have been studied extensively both by experimentalists and theoreticians due to their molecular structure allowing for computationally inexpensive simulations of optical and electronic properties that can then be tested easily in the laboratory, both in solution and the solid state. Their rigidity allows for controllable adjustment of molecular parameters such as aromaticity and conjugation length without having to account for multiple conformations as often encountered in the crystal structures of non-rigid molecules<sup>1</sup>. They have a strong propensity toward crystallisation as a result of two intermolecular bonding mechanisms. Charge is concentrated toward the centre of the aromatic moiety, leaving peripheral atoms electropositive which can then interact with carbon atoms on adjacent molecules, encouraging edge-face interactions. This competes with  $\pi$ -stacking interactions between aromatic rings in neighbouring molecules that arise as a result of dispersion forces and electrostatic quadrupole interactions between delocalised electrons in p-orbitals which encourage parallel stacking<sup>2</sup>. These two competing processes can clearly be seen in the crystal structure of coronene (Fig. 1), which adopts a herringbone motif with clear edge-face C-H and layered  $\pi$ -stacking C-C interactions. In the gamma-herringbone polymorph, the C-H interactions are dominant, whereas in the beta-herringbone configuration there is strong  $\pi$ - $\pi$  overlap with minimal C-H bonding<sup>3</sup>. A recently synthesised variant of coronene, persulfurated coronene (2<sup>nd</sup> generation sulflower, or PSC)<sup>4</sup>, in which all hydrogen atoms have been substituted with sulfurs (see SI fig. 1 for structural formula), has not been found to form an ordered crystalline state, a phenomenon which has been examined

through multiple growth techniques as well as differential scanning calorimetry (DSC), X-ray diffraction (XRD) and electron diffraction (ED). Computational optimisations of molecules suggest that PSC molecules almost exclusively favour direct stacking interactions, which are not conducive to crystal formation.

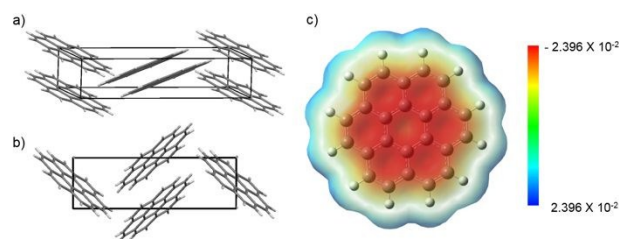


Fig. 1: a) beta and b) gamma polymorphs of coronene, viewed slightly offset from the a and c axes and down the a axis respectively. c) Electrostatic potential map of a coronene molecule. Units in e/Å.

PSC was provided from the University of Dresden as a brown granular powder and used as received. Powder XRD resulted in a generally flat pattern with two broad peaks at  $2\theta = 8.31^\circ$  and  $25.55^\circ$  (SI Fig. 2). Solubility tests showed that of all solvents tested (NMP, DMF, DMSO, toluene, ethyl acetate, THF), the only solvent in which PSC was soluble to a concentration greater than 1 mg per ml was NMP. PSC was therefore dissolved in NMP at 80 °C until no more could be dissolved. The solution was then filtered and cooled to 0 °C over 1 hour. All material remained in solution after the temperature ramp was completed. Dropcasting of the 80 °C solution onto a glass slide cooled to -4 °C resulted in the formation of aggregates approximately 2 mm in size, but powder and single crystal XRD of these aggregates revealed them to be amorphous (SI Fig. 3). In a second method, physical vapour transport growth was attempted at both ambient pressure in a glass tube with a 0.1 L/min nitrogen flow across the tube. PSC powder was positioned at the centre of a tube furnace heated to 250 °C, with a temperature of 100 °C at either end with an approximately consistent temperature gradient between the centre and edge. This resulted in a black residue at the point of sublimation, and an amorphous brown lining on the

<sup>a</sup> School of Chemistry, University of Bristol, Cantock's Close, Bristol BS8 4ND

<sup>b</sup> Istituto Italiano di Tecnologia, Center for Nanotechnology Innovation @ NEST, Piazza San Silvestro 12, 56127 Pisa, Italy

Electronic Supplementary Information (ESI) available: See DOI: 10.1039/x0xx00000x

glass 10 cm from the sublimation point. This was repeated in a vacuum sealed ampoule, similarly producing an amorphous lining and residue indicating decomposition of the PSC. DSC data on the raw powder was collected by subjecting a hermetically sealed pan containing 2.8 mg of PSC to a heating and cooling cycle between  $-70\text{ }^{\circ}\text{C}$  and  $300\text{ }^{\circ}\text{C}$ , and from  $300\text{ }^{\circ}\text{C}$  to  $-70\text{ }^{\circ}\text{C}$  at a rate of  $10\text{ }^{\circ}\text{C}/\text{min}$

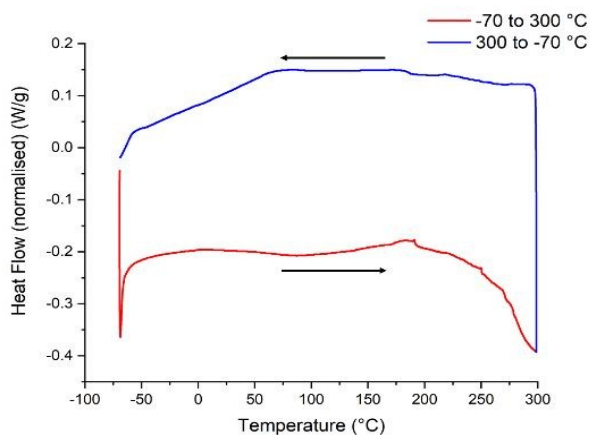


Fig. 2: Differential scanning calorimetry data for PSC

(Fig. 2). The measured relative heat flow in or out of the material as a function of temperature clearly shows no crystallisation events over the run; the only features present are a broad endothermic valley between  $200\text{ }^{\circ}\text{C}$  and  $300\text{ }^{\circ}\text{C}$  as a result of partial sublimation of the material and a linear endothermic transition during cooling which is a function of the cooling rate applied to the material. In order to ensure that there were no crystalline domains of any size in PSC, the crystallinity was analysed at the nanoscale through the collection of electron diffraction data from different areas of the same sample (Fig. 3). High angle annular dark-field scanning transmission electron microscopy (HAADF-STEM) imaging, EDS and ED data were recorded with a Zeiss Libra TEM operating at  $120\text{ kV}$  and equipped with a  $\text{LaB}_6$  source and a Bruker EDS detector XFlash6T-60. ED patterns were collected in Köhler parallel illumination with a beam size of about  $150\text{ nm}$  in diameter

obtained using a  $5\text{ }\mu\text{m}$  C2 condenser aperture and recorded by an ASI MEDIPIX detector<sup>5</sup>, which is able to record the arrival of single electrons and deliver virtually background-free patterns. With such a detector it is possible to record diffraction patterns with doses of approximately  $0.01\text{ el } \text{\AA}^{-2}$  avoiding beam amorphization of beam sensitive samples. A few grains of as-received PSC were gently

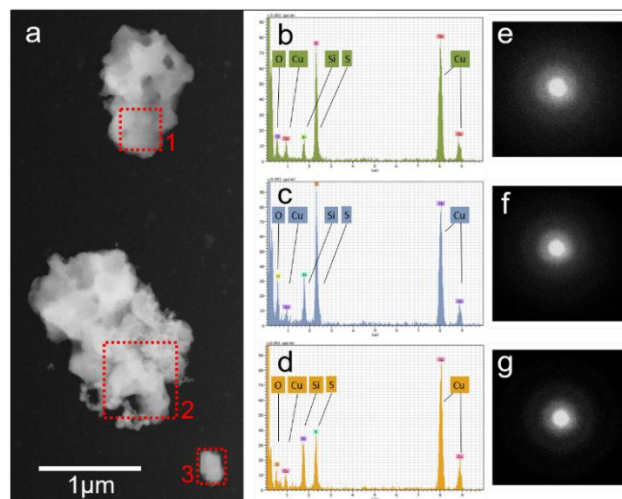


Fig. 3: (a) STEM overview. (b, c, d) EDS spectra from areas 1, 2, 3 in (a). Cu, Si, O signals come from grid and detector. (e, f, g) ED patterns from areas 1, 2, 3 in (a)

crushed and directly loaded on a carbon-coated Cu TEM grid without any solvent or sonification. The sample forms aggregates of a few  $\mu\text{m}$  in size (Fig. 3a). Energy dispersive X-ray spectroscopy (EDS) spectra (Fig. 3b-d) were collected from selected areas on three different aggregates. In all cases, EDS spectroscopy reveals the presence of sulfur (S). The S:C ratio could not be measured as the carbon (C) signal could not be quantified. ED data collected by TEM from these areas did not show any Bragg reflection or other hint of crystallinity (Fig. 3e-g). The only features in diffraction are diffuse rings consistent with an amorphous state. The patterns have been collected under extremely low dose conditions with a total dose of  $0.01\text{ el } \text{\AA}^{-2}$  to avoid any beam damage.

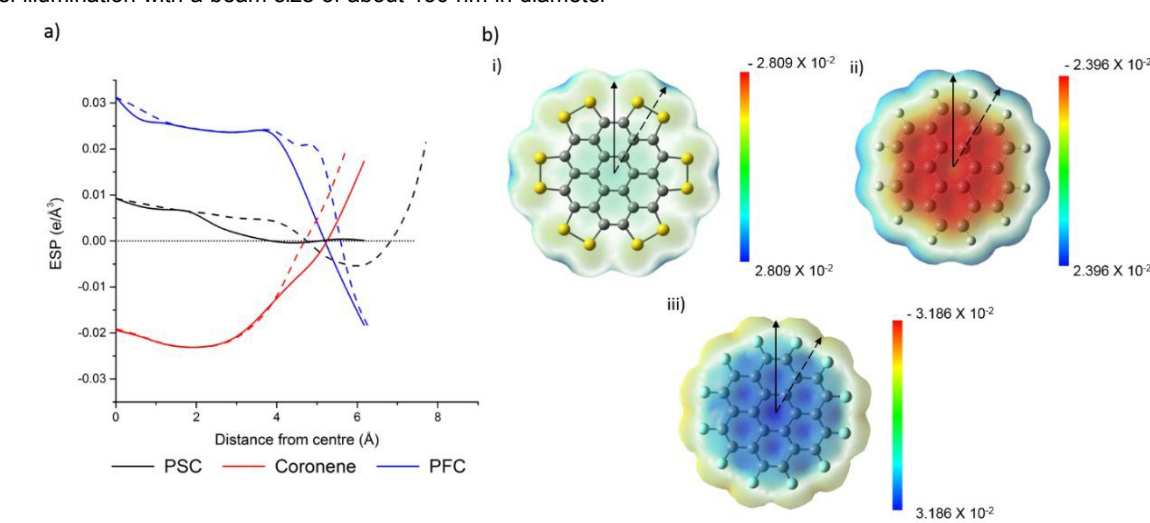


Fig. 4: Calculated electrostatic potential across perfluorinated coronene, coronene and persulfurated coronene in a line from the centre of the molecule to the edge down the centre of the anthracene constituent (solid) and along the radial carbon-carbon bond (dashed). b) Full electrostatic potential map of i) persulfurated coronene, ii) coronene and iii) perfluorinated coronene. Units in  $\text{e}/\text{\AA}$ .

The number of rotatable bonds in an organic molecule is a key descriptor in its likelihood to crystallise, with molecules that possess a greater number being less likely to form high quality crystals. However, PSC has no rotatable bonds and so its reticence to crystallise must lie in its charge distribution<sup>6</sup>. Electrostatic potential calculations were performed on a molecule of PSC via DFT with a B3LYP functional and 6-31G (d,p) basis set in the Gaussian software package<sup>7</sup> (Fig. 4bi). This shows a broadly flat distribution of charge across the molecule, with positive pockets on the periphery of the sulfur atom pairs. The difference in charge density between the centre of the molecule and the edge varies between 0.0093 and 0.0211 e/Å. In coronene, this difference is far greater, with the centre and edge of the molecule possessing an ESP of -0.0224 and the 0.0200 e/Å respectively (Fig. 4bii). Perfluorinated

Desiraju and Gavezzotti stated that, in the case of polyaromatic hydrocarbons (PAHs), the crucial link between molecular and crystal structure is the relative ability of a molecule to employ C-C and C-H interactions. They then state that it may be expected that the effect on crystal structure should be the same whenever similar molecular shapes are found in organic compounds which are not purely hydrocarbons<sup>8</sup>. Examining this in the case of sulflower, a planar, rotationally symmetrical molecule comprised purely of carbon and sulfur similar to PSC, a crystal structure has been obtained via a combination of experimental data and theoretical fitting<sup>9</sup>. Sulflower also has a similar electrostatic potential surface to PSC, with charge distributed equally on the faces of the molecule (fig. 5). However, positive regions appear on the edges between the sulfur atoms as charge is pulled toward the C-S bonds on either

Dimer	Mode	Distance (Å)	Offset (Å)	Torsion (°)	Energy (kJ.mol <sup>-1</sup> )			
					E.S.	Rep.	Disp.	Total
Coronene	Offset	3.499	1.376	0	8.8	60.7	-162.2	-92.8
	Twisted	3.538	0	30	12.8	69.2	-164.2	-92.2
Sulflower	Offset	3.538	1.231	0	2.5	61.5	-158.3	-94.3
	Twisted	3.569	0	22.5	2.2	65.8	-166.6	-98.6
PSC	Offset	3.535	1.293	0	-2.1	105.2	-267.4	-164.3
	Twisted	3.538	0	16.25	-5.7	108.8	-257.4	-172.0

Table 1: Parameters of the two dimer conformations of coronene, sulflower and PSC with their associated potentials and the electrostatic, repulsion and dispersion contributions.

coronene (PFC), in which the hydrogen atoms of coronene have been substituted for fluorine atoms, possesses a similar planar molecular structure to coronene but the distribution of charge is reversed as negative charge is redistributed to the edge of the molecule leaving the core highly electropositive (Fig. 4biii). The centre and edge of the molecule have ESPs of 0.0310 and -0.0186 e/Å respectively. It therefore appears that the sulfur atoms of PSC strike a balance between hydrogen and fluorine, resulting in a generally homogeneous charge distribution. Measuring the ESP in a line from the centre of each molecule to the edge through the anthracene constituent and the radial carbon-carbon bond (Fig. 4a), it can be seen that for coronene and PFC there are stark differences in the charge at the centre compared to the edge, whereas with PSC there is little charge at the centre. This means that for PSC, no attractive interactions can take place between the edge and centre of the molecule.

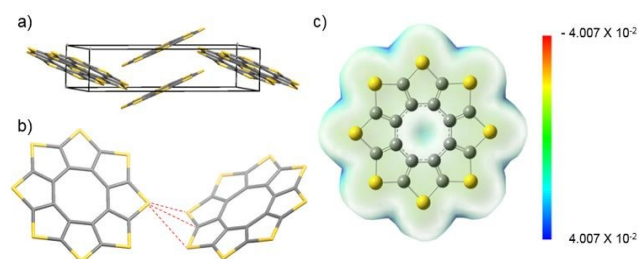


Fig. 5: a) Crystal structure of sulflower viewed slightly offset from the b and c axes. b) interaction between sulflower molecules in neighbouring  $\pi$ -stacks. c) ESP map of a sulflower molecule. Units in e/Å.

side. These regions interact with the protruding sulfur atoms, allowing for edge-face interactions between molecules in adjacent  $\pi$ -stacks. This bonding motif is weak compared to the dominant C-C interactions down the stacks, resulting in a short axis of 3.89 Å and a nearest neighbour angle of 47.51°, placing it within the  $\beta$  family of crystal structures and demonstrating that the statement holds true<sup>2</sup>. The hypothesis breaks down with PSC however, as although there are also positively charged regions around the edge of the molecule they are of lesser magnitude and the molecular geometry is such that the sulfur atoms cannot interact with these regions, suggesting that edge-face interactions which are critical for crystal formation are not feasible under normal conditions.

The preferred stacking conformations of coronene, sulflower and PSC were examined by performing a series of 100 two-molecule optimisations in the ORIENT software package<sup>10</sup>, in which the two molecules were positioned randomly in space, which converged to the optimum packing modes of the molecular dimer at 0 K (SI fig.



4). All three dimers exhibit two minima: an offset stacking mode in which the molecules are aligned, and a direct stacking mode with the molecules twisted by a specific torsion angle (known as the "twisted sandwich" mode<sup>11</sup>). The twisted stacking mode is more stable than the offset stack for PSC and sulflower (Table 1), with the greatest difference in energy between PSC modes (4.3 kJ.mol<sup>-1</sup> for sulflower and 7.7 kJ.mol<sup>-1</sup> for PSC). For coronene, the offset stack is more stable by 0.6 kJ.mol<sup>-1</sup>, suggesting that thermal effects would be sufficient for the dimers to transition between the two forms. PSC is the only case in which the electrostatic interaction contributes constructively to the stability of the conformations. The interaction potentials are nearly twice as strong for PSC as they are for sulflower and coronene, suggesting a greater propensity toward face-face stacking. To test this further, 100 three-molecule optimisations were examined, resulting in several different modes with various combinations of face-face and edge-face interactions (SI fig. 5). The direct stacking mode in PSC is the most favourable for all numbers of molecules tested, with conformations featuring edge-face interaction approximately 0.65 times as stable and with a difference of 125 kJ.mol<sup>-1</sup>. The coronene trimers all formed into two configurations: all three offset-stacked, and two offset-stacked with the face of the third molecule interacting with the edge similar to the gamma polymorph. Over 100 calculations of each number of molecules, no direct stacking between coronene molecules was observed, suggesting that this mode is at least unlikely to manifest in pre-nucleation clusters. Direct stacking of aromatic rings is highly uncommon in crystal structures<sup>12</sup>, and does not appear to be conducive toward crystal formation. Direct stacking of greater than two molecules would lead to large, energetically unfavourable unit cells which could not be categorised into any of the known crystal structures of planar aromatic molecules<sup>2</sup>. These results were confirmed by calculating the potential landscapes of dimers of PSC, coronene and sulflower in edge-face and face-face configurations in the x-y plane at constant z separation (SI fig. 6) which suggest that face-face interactions are approximately five times stronger than edge-face interactions in PSC, whereas for coronene these values are much closer. Given the stability of direct stacked clusters of PSC molecules relative to those with edge-face interactions, it may therefore be that such structures are forming in pre-nucleation clusters and are unable to then transition to a configuration that would enable the formation of crystals under the conditions tested. The broad peaks in the XRD pattern of PSC (SI Fig. 2) at 25.55° and 8.31° correspond to d-spacings of 3.48 Å and 10.63 Å respectively, which match closely with the optimised distance between two and four stacked PSC molecules. The presence of only two peaks suggests that the formation of one-dimensional columnar structures of PSC molecules in the twisted-stack motif is more likely than offset stacking.

In conclusion, the planar aromatic molecule persulfurated coronene could not be crystallised via solvent growth, PVT under ambient and vacuum conditions, and dropcasting. Electron diffraction confirms that aggregates of this molecule are amorphous under vacuum, even at the nanoscale. ESP calculations on PSC show that it has a broadly homogeneous charge distribution, and this along with its molecular geometry mean that edge-face interactions between molecules are at least highly unfavourable, with optimisation calculations always favouring direct face-face

interactions. Powder XRD on aggregates under ambient conditions likely show the presence of face-face stacks of PSC molecules. This is the first reported planar aromatic molecule that appears to break with conventions of crystallisation which have held true for all such molecules. However, achieving nucleation in this molecule may yet be possible via methods which attain high supersaturation over greater periods of time, including gel-based diffusion methods. PSC provides an interesting model for computational study and could aid in the design of molecules in which crystallisation is directed toward specific interactions, for example in liquid crystals in which face-face stacking is desired. This is normally achieved by adding long alkyl chains to an aromatic core<sup>13</sup>, but this discovery may provide an easier route to achieving such systems with relatively simple molecular design. Much research has also been done on molecular glasses which could potentially combine the processability and quick preparation of polymers with the ease of purification and the high carrier mobilities of single crystals. The encouragement of glass formation is usually achieved via the addition of bulky substituents to a base molecule<sup>14</sup>, however this manuscript shows that the prevention of crystallisation may also be achieved in smaller molecules if the molecular charge distribution is carefully considered.

S.R.H., T.T.J. and C.L.H. acknowledge the Engineering and Physical Sciences Research Council UK (grant EP/G036780/1) and the Centre for Doctoral Training in Condensed Matter Physics for project funding. S.R.H. and J.P. acknowledge MagnaPharm, a collaborative research project funded by the European Union's Horizon 2020 Research and Innovation programme (grant No. 736899). All researchers thank Dr Xinliang Feng and Prof Klaus Muellen for generously providing the persulfurated coronene for this research, and Dr Hazel Sparkes for XRD data collection of the raw PSC powder.

## References

- 1 R. Rieger and K. Müllen, *J. Phys. Org. Chem.*, 2010, **23**, n/a-n/a.
- 2 G. R. Desiraju and A. Gavezzotti, *Acta Crystallogr. Sect. B*, 1989, **45**, 473–482.
- 3 J. Potticary, L. R. Terry, C. Bell, A. N. Papanikolopoulos, P. C. M. Christianen, H. Engelkamp, A. M. Collins, C. Fontanesi, G. Kociok-Köhn, S. Crampin, E. Da Como and S. R. Hall, *Nat. Commun.*, 2016, **7**, 11555.
- 4 R. Dong, M. Pfeffermann, D. Skidin, F. Wang, Y. Fu, A. Narita, M. Tommasini, F. Moresco, G. Cuniberti, R. Berger, K. Müllen and X. Feng, *J. Am. Chem. Soc.*, 2017, **139**, 2168–2171.
- 5 D. Georgieva, J. Jansen, I. Sikharulidze, L. Jiang, H. W. Zandbergen and J. P. Abrahams, *J. Instrum.*, 2011, **6**, C01033–C01033.
- 6 J. G. P. Wicker and R. I. Cooper, *CrystEngComm*, 2015, **17**, 1927–1934.
- 7 M. J. Frisch et al, Gaussian 16, Revision C.01, Gaussian, Inc., Wallingford CT, 2016.
- 8 G. R. Desiraju and A. Gavezzotti, *J. Chem. Soc. Chem. Commun.*, 1989, 621–623.
- 9 K. Y. Chernichenko, V. V. Sumerin, R. V. Shpanchenko, E.

## Journal Name

## COMMUNICATION

- S. Balenkova and V. G. Nenajdenko, *Angew. Chemie*, 2006, **118**, 7527–7530.
- 10 D. R. Stone et al, Nutt and D. J. Popelier, P. L. A., Wales, Orient version 5.0, University of Cambridge, 2018.
- 11 O. I. Obolensky, V. V. Semenikhina, A. V. Solov'yov and W. Greiner, *Int. J. Quantum Chem.*, 2007, **107**, 1335–1343.
- 12 M. O. Sinnokrot and C. D. Sherrill, *J. Phys. Chem. A*, 2006, **110**, 10656–10668.
- 13 M. Gingras, J.-M. Raimundo and Y. M. Chabre, *Angew. Chemie Int. Ed.*, 2006, **45**, 1686–1712.
- 14 P. Strohriegl and J. V. Grazulevicius, *Adv. Mater.*, 2002, **14**, 1439–1452.

View Article Online  
DOI: 10.1039/C9CC08346D

**Competing Interests**

The Authors declare that they have no competing interests.